Articles

Salts Induce Structural Changes in Elongation Factor 1α from the Hyperthermophilic Archaeon *Sulfolobus solfataricus*: A Fourier Transform Infrared Spectroscopic Study[†,‡]

Fabio Tanfani,[§] Andrea Scirè,[§] Mariorosario Masullo,*[,||,⊥] Gennaro Raimo,[||] Enrico Bertoli,[@] and Vincenzo Bocchini[||]

Istituto di Biochimica, Facoltà di Scienze Matematiche, Fisiche e Naturali, and Facoltà di Medicina e Chirurgia, Università degli Studi di Ancona, Via Ranieri, I-60131 Ancona, Italy, Dipartimento di Biochimica e Biotecnologie Mediche, Università degli Studi di Napoli Federico II, Via S. Pansini 5, I-80131 Napoli, Italy, and Dipartimento di Scienze Farmacobiologiche, Università degli Studi di Catanzaro Magna Graecia, Complesso Ninì Barbieri, Roccelletta di Borgia, I-88021 Catanzaro, Italy

Received January 19, 2001; Revised Manuscript Received July 27, 2001

ABSTRACT: Elongation factor 1α from the hyperthermophilic archaeon *Sulfolobus solfataricus* (*Ss*EF-1α) carries the aminoacyl tRNA to the ribosome; it binds GDP or GTP, and it is also endowed with an intrinsic GTPase activity that is triggered in vitro by NaCl at molar concentrations [Masullo, M., De Vendittis, E., and Bocchini, V. (1994) *J. Biol. Chem. 269*, 20376−20379]. The structural properties of *Ss*EF-1α were investigated by Fourier transform infrared spectroscopy. The estimation of the secondary structure of the *Ss*EF-1α·GDP complex, made by curve fitting of the amide I′ band or by factor analysis of the amide I band, indicated a content of 34−36% α-helix, 35−40% β-sheet, 14−19% turn, and 7% unordered structure. The substitution of the GDP bound with the slowly hydrolyzable GTP analogue Gpp(NH)p induced a slight increase in the α-helix and β-sheet content. On the other hand, the α-helix content of the *Ss*EF-1α·GDP complex increased upon addition of salts, and the highest effect was produced by 5 M NaCl. The thermal stability of the *Ss*EF-1α·GDP complex was significantly reduced when the GDP was replaced with Gpp(NH)p or in the presence of NaBr or NH_4Cl, whereas a lower destabilizing effect was provoked by NaCl and KCl. Therefore, the extent of the destabilizing effect of salts depended on the nature of both the cation and the anion. The data suggested that the sodium ion was responsible for the induction of the GTPase activity, whereas the anion modulated the enzymatic activity through destabilization of particular regions of *Ss*EF-1α. Finally, the infrared data suggested that, in particular region(s) of the polypeptide chain, the *Ss*EF-1α·Gpp(NH)p complex possesses structural conformations which are different from those present in the *Ss*EF-1α·GDP complex.

During the elongation cycle in the process of protein synthesis in the hyperthermophilic archaeon *Sulfolobus solfataricus*, elongation factor 1α (*Ss*EF-1α)[1] bound to GTP catalyzes the binding of aminoacyl-tRNA to the ribosome (*1*−*3*). Following the interaction of *Ss*EF-1α with the ribosome, the intrinsic GTPase of the elongation factor is unmasked and the hydrolysis of the bound GTP generates an inactive *Ss*EF-1α·GDP complex that delivers the aa-tRNA to the A site and leaves the ribosome. *Ss*EF-1α is constituted by three putative structural domains (*4*) that have been identified on the basis of the alignment of its primary structure with that of the eubacterial analogue EF-Tu, whose three-dimensional (3D) structure in complex with different ligands is well-known (*5*−*8*). Domain I is the catalytic domain and contains the nucleotide binding site; domain II regulates the affinity for the nucleotides and the thermophilicity of *Ss*EF-1α, whereas domain III is essential for protein synthesis and is involved in the thermostability of the factor. *Ss*EF-1α is a very thermostable and thermoactive GTP-binding protein (*1*, *9*), and as such, it elicits an intrinsic GTPase that is triggered by sodium ions (*10*). The stimulatory effect is regulated by the anion, and the most effective triggering system is constituted by NaCl at molar concentra-

[†] This work was supported by grants from Ancona University (F.T. and E.B.), EU Biotech Programme Contract BIO4-CT97-2188 (V.B.), and Consiglio Nazionale delle Ricerche, Rome, Italy (V.B.).

[‡] This paper is dedicated to the memory of Prof. Vincenzo Bocchini.

* To whom correspondence should be addressed: Dipartimento di Biochimica e Biotecnologie Mediche, Università degli Studi di Napoli Federico II, Via S. Pansini 5, I-80131 Napoli, Italy. Telephone: +39 081 7463118. Fax: +39 081 7463653. E-mail: masullom@dbbm.unina.it.

[§] Istituto di Biochimica, Facoltà di Scienze Matematiche, Fisiche e Naturali, Università degli Studi di Ancona.

[||] Università degli Studi di Napoli Federico II.

[⊥] Università degli Studi di Catanzaro Magna Graecia.

[@] Facoltà di Medicina e Chirurgia, Università degli Studi di Ancona.

[1] Abbreviations: *Ss*, *S. solfataricus*; EF-, elongation factor; $GTPase^{Na}$, *Ss*EF-1α GTPase triggered by sodium ions; FT-IR, Fourier transform infrared; amide I′, amide I band in a ^2H_2O medium; T_m, temperature for half-denaturation; Gpp(NH)p, guanyl-5′-yl imido diphosphate, a slowly hydrolyzable analogue of GTP.

10.1021/bi0101291 CCC: $20.00
Published on Web 10/11/2001

tions in the presence of Mg^{2+} or Mn^{2+} at millimolar concentrations (*10*). Because only preliminary information is available for the 3D structure of *Ss*EF-1α (unpublished results), we have studied the secondary structure and the thermal stability of *Ss*EF-1α in the GDP- or Gpp(NH)p-bound form by Fourier transform infrared spectroscopy. In addition, to gain insight into the mechanism of the stimulatory effect exerted by NaCl, we have investigated the effect of this salt on the structural properties of the *Ss*EF-1α·GDP complex. The comparison of the effect produced by other salts on the structural properties of the *Ss*EF-1α·GDP complex allowed identification of the different effect exterted by the anion and the cation.

MATERIALS AND METHODS

Materials. Deuterium oxide (99.9% ^2H_2O), ^2HCl, and NaO^2H were purchased from Aldrich. GDP, Gpp(NH)p, and Tris were obtained from Sigma. All the other chemicals were of the purest quality. *S. solfataricus* EF-1α was isolated from an *Escherichia coli* strain as previously reported (*11*). *Ss*EF-1α·GDP and *Ss*EF-1α·Gpp(NH)p complexes were prepared starting from the *Ss*EF-1α nucleotide free as previously reported (*12*). The purity of all protein samples was assessed by SDS−PAGE, and their specific activity was tested at 60 °C by either [^{3}H]GDP binding (*1*) or GTPase^{Na} (*10*).

Preparation of Samples for Infrared Measurements. Protein (1−1.5 mg) dissolved in 300 μL of 20 mM Tris-HCl buffer (pH 7.8), 2 mM $MgCl_2$ (buffer A), 1 mM GDP, or 1 mM Gpp(NH)p was concentrated in a Centricon 10 microconcentrator (Amicon) at 3000*g* and 4 °C. Buffer A (300 μL) containing the appropriate guanine nucleotide, prepared in H_2O or ^2H_2O (pH or p^{2}H 7.8, respectively), was added and the sample concentrated again. The p^{2}H value equals the pH meter reading + 0.4 (*13*). The concentration and dilution procedure was repeated several times to completely replace the original buffer with buffer A containing GDP or Gpp(NH)p. For the experiments in the presence of different salts, the *Ss*EF-1α·GDP complex was treated as reported above with buffer A containing 1 mM GDP at p^{2}H 7.8 containing one of the following salts: 2.5 or 5 M NaCl, 2.5 M KCl, 2.5 M NH_4Cl, or 2.5 M NaBr. For each sample, the whole procedure took 24 h, which was the time of contact of the protein with the ^2H_2O medium prior to FT-IR analysis. In the last concentration step, the sample was brought to a final volume of approximately 40 μL, a volume useful for infrared measurements.

Infrared Spectra. The concentrated sample was placed in a thermostated Graseby Specac 20500 cell (Graseby-Specac Ltd., Orpington, Kent, U.K.) fitted with CaF_2 windows and 6 or 25 μm spacers for measurements in H_2O or ^2H_2O, respectively. FT-IR spectra were recorded by a Perkin-Elmer 1760-x Fourier transform infrared spectrometer using a deuterated triglycine sulfate detector and a normal Beer-Norton apodization function. At least 24 h in advance, and during data acquisition, the spectrometer was continuously purged with dry air at a dew point of −40 °C. Spectra were acquired at 2 cm^{-1} resolution, and blanks run in the absence of protein were subtracted. Usually, 256 scans were averaged for each spectrum obtained at 20 °C, while 16 scans were averaged for spectra obtained at higher temperatures. In this last case, the temperature was increased by 5 °C steps up to 95 °C, and then other two spectra were collected at 98 and 99 °C. Before spectrum acquisition, samples were maintained at the desired temperature for a 6 min time interval that is necessary for the stabilization of temperature inside the cell. Spectra were processed using the SPECTRUM software from Perkin-Elmer. Correct subtraction of the H_2O absorption from the sample spectrum yielded an approximately flat baseline in the 1900−1400 cm^{-1} interval (*14*). Subtraction of the ^2H_2O absorption was corrected to the removal of the ^2H_2O bending absorption close to 1220 cm^{-1} (*14*). The deconvoluted parameters for the amide I band were set to a γ value of 2.5 and a smoothing length of 60. Second-derivative spectra were calculated over a nine-data point range (9 cm^{-1}).

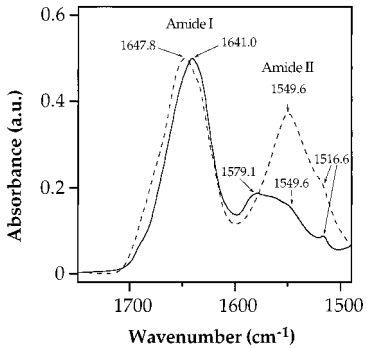

FIGURE 1: Absorbance FT-IR spectra of the *Ss*EF-1α·GDP complex. Solid and dashed lines represent spectra at 20 °C of the *Ss*EF-1α·GDP complex in ^2H_2O and H_2O, respectively. Spectra were normalized to the same amide I band height.

The estimation of the secondary structure composition was obtained by curve fitting of the deconvoluted amide I′ band as reported previously (*15*) and using the software GRAMS 32 (Galactic Industries Corp.).

The estimation of the secondary structure composition was also obtained by factor analysis of the infrared spectrum of the *Ss*EF-1α·GDP complex in H_2O (*16*).

RESULTS

Secondary Structure Analysis of Nucleotide-Bound SsEF-1α. The IR absorbance spectra of *Ss*EF-1α·GDP in H_2O or ^2H_2O in the region of 1750−1500 cm^{-1} are reported in Figure 1. In H_2O, the spectrum is characterized by the amide I band with a maximum at 1647.8 cm^{-1} and by the amide II band with a maximum located at 1549.6 cm^{-1}. In ^2H_2O, the amide I band (amide I′) is shifted to 1641 cm^{-1} and the amide II band intensity decreased significantly, as a consequence of its shift to ∼1450 cm^{-1} (not shown). The other absorption bands are due to amino acid side chains, and in particular, the 1516.6 and 1579.1 cm^{-1} bands were due to tyrosine and ionized aspartic acid, respectively (*17*). These phenomena observed with proteins in ^2H_2O were due to the hydrogen exchange of the NH amide with deuterium (^{1}H−^{2}H) (*18*). The deconvoluted spectrum of *Ss*EF-1α in H_2O displayed bands at 1698.3, 1690.5, 1674.9, 1655.2, 1647.8, 1634.2, and 1621 cm^{-1} (not shown).

The amide I′ band components were identified in peaks and shoulders in the deconvoluted spectra of the *Ss*EF-1α·GDP complex (Figure 2A) and the *Ss*EF-1α·Gpp(NH)p complex (not shown) in ^2H_2O. Figure 2B shows that the second-derivative spectra of both complexes are very similar and the same amide I′ band components are located almost in the same positions. The presence of α-helix and β-sheet

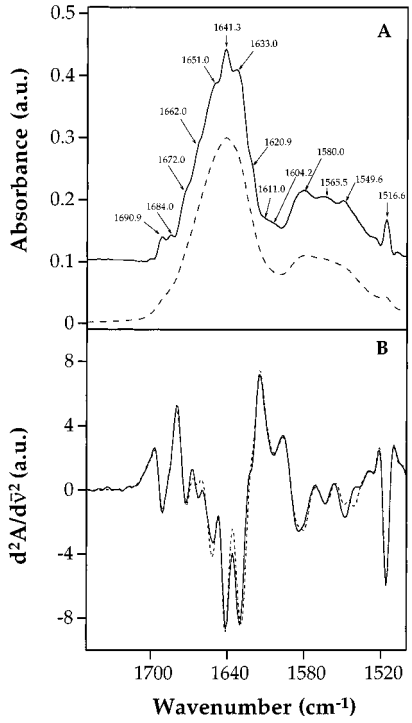

FIGURE 2: Absorbance, deconvoluted, and second-derivative spectra of nucleotide-bound *Ss*EF-1α in ^2H_2O at 20 °C. (A) The absorbance spectrum of the *Ss*EF-1α·GDP complex (dashed line) was that reported in Figure 1; the deconvoluted spectrum (solid line) is the result of a mathematical treatment for identification of the amide I band components and amino acid side chain absorption. (B) Second-derivative spectra of the *Ss*EF-1α·GDP complex (solid line) and the *Ss*EF-1α·Gpp(NH)p complex (dotted line) were superimposed. For other details, see Materials and Methods.

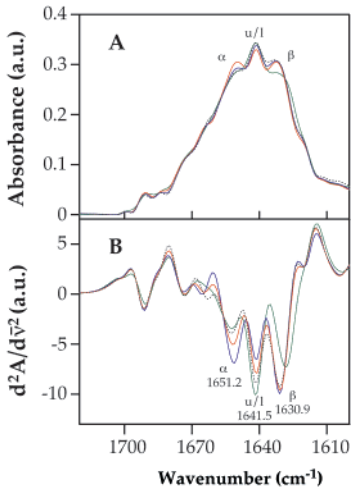

FIGURE 3: Deconvoluted (A) and second-derivative spectra (B) of the *Ss*EF-1α·GDP complex in the absence or presence of NaCl at different concentrations, at 20 °C. Dotted black, red, and blue curves represent the spectra of the *Ss*EF-1α·GDP complex in the presence of 0, 2.5, and 5 M NaCl, respectively. The spectrum of the *Ss*EF-1α·Gpp(NH)p complex is shown in green. The symbols α, *β*, and u/l stand for α-helix, *β*-sheet, and unordered structures and/or loops, respectively.

structures in both complexes was revealed by the bands close to 1651 and 1633 cm^{-1}, respectively (*19*). The 1620.9 cm^{-1} band could be due to *β*-sheet particularly exposed to the solvent (*20*) and/or to amino acid side chain absorption (*17*). Other *β*-sheet bands were those at 1690.9 (*13*, *14*) and 1684 cm^{-1}, although the latter band may also be due to turns (*21*). The presence of both the 1633 and 1684 cm^{-1} bands suggests that *β*-sheets are antiparallel (*20*). The 1672 and 1662 cm^{-1} bands were assigned to turns, and the 1641.3 cm^{-1} band was assigned to loops and/or unordered structures (*19*, *22*). The position of the latter band is found at a wavenumber shorter than the averaged position for an unordered structure band that is located at ∼1645 cm^{-1} (*19*, *23*). This finding has already been reported for lysozyme (*23*) and for the random conformation of poly(L-lysine) (*24*).

It should be mentioned also that α-helices and coiled coils have been reported to exhibit in ^2H_2O a band at ∼1640 cm^{-1} (*24*−*27*). However, the comparison between the spectra reported in these references and those of *Ss*EF-1α allowed the assignment of the 1641.3 cm^{-1} band to unordered structures and/or loops. The other bands reported in Figure 2 were due to the absorption of amino acid side chains (*17*). In addition, the 1549.6 cm^{-1} band represents a residual amide II absorption, thus indicating that ^2H_2O cannot reach all the protein segments at 20 °C (*18*).

With regard to the *Ss*EF-1α·Gpp(NH)p complex, a significantly higher content of α-helix, compared to that of the *Ss*EF-1α·GDP complex, was found (Figure 2B). With regard to the *β*-structure content, almost no variation in the intensity of the corresponding bands was observed, although some of them were shifted toward shorter wavenumbers. This last finding indicated that these *β*-structure elements exchanged more easily ^1H for ^2H and therefore could be more exposed to the solvent compared to those of the *Ss*EF-1α·GDP complex (*18*).

Salt-Induced Structural Changes in the SsEF-1α·GDP Complex. The deconvoluted spectra in Figure 3A showed that NaCl induces changes in the secondary structure of the *Ss*EF-1α·GDP complex as indicated by the different intensities of the amide I′ band components. These changes were much more evident in the second-derivative spectra (Figure 3B) that amplify changes in the curve slope (*28*). In particular, NaCl increased the intensity of the α-helix band (1651−1652 cm^{-1}) and decreased the intensity of the band due to loops and/or unordered structures (1641.5 cm^{-1}). In the case of the *Ss*EF-1α·Gpp(NH)p complex, the addition of 5 M NaCl did not provoke significant alterations in the spectrum (Figure 3). Other minor changes involved the *β*-turn band, which was shifted to higher wavenumbers, and the *β*-sheet band. With regard to the *Ss*EF-1α·GDP complex, the effect produced by NaCl was similar to that obtained with NaBr, NH_4Cl, and KCl (Figure 4). In particular, NaBr and NH_4Cl provoked changes in the secondary structure of the protein similar to those provoked by NaCl, whereas KCl produced a minor effect.

To estimate the content in the secondary structure of the *Ss*EF-1α·GDP complex and the structural changes provoked by salts, a curve fitting of the deconvoluted amide I′ band was performed (*15*). The results reported in Table 1 showed that in the absence of salts, the α-helix and *β*-sheet contents of the *Ss*EF-1α·GDP complex were similar (36 and 35%, respectively), as obtained from the two main bands close to 1651 and 1631 cm^{-1}, respectively. However, if the contribution to the *β*-sheet content due to the 1684 and 1619 cm^{-1} bands was also considered, the total content of *β*-sheets increased slightly. This finding is in line with the estimation of the secondary structure obtained by factor analysis of the infrared spectrum of the *Ss*EF-1α·GDP complex in H_2O

Table 1: Calculated Positions and Fractional Areas (%) of the Amide I′ Component Bands for *Ss*EF-1α at 20 °C in the Absence or Presence of Different Salts

	Gpp(NH)p bound		GDP bound					
band position (cm^{-1})	no salt (%)	5 M NaCl (%)	no salt (%)	2.5 M NaCl (%)	5 M NaCl (%)	2.5 M KCl (%)	2.5 M NaBr (%)	2.5 M NH_4Cl (%)
1691 (*β*)	1	2	1	1	2	1	1	1
1684 (*β*/t)	2	1	2	2	2	2	3	2
1673 (t)	8	7	6	6	7	3	7	7
1664 (t)	7	8	11	8	6	14	7	7
1651 (α)	38	39	36	45	48	38	40	41
1641 (u/l)	6	7	7	4	3	5	4	4
1631 (*β*)	37	35	35	32	29	35	36	36
1619 (*β*/aa)	1	1	2	2	3	2	2	2

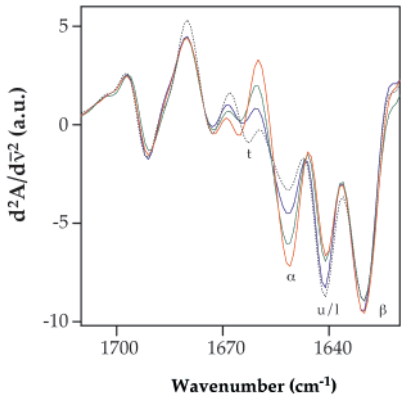

FIGURE 4: Second-derivative spectra of the *Ss*EF-1α·GDP complex at 20 °C in the absence or presence of NaBr, NH_4Cl, or KCl. Dotted black, red, green, and blue curves represent the spectra of the *Ss*EF-1α·GDP complex without added salt and in the presence of 2.5 M NaBr, NH_4Cl, and KCl, respectively. The symbols α, *β*, and u/l are defined in the legend of Figure 3; t stands for turns.

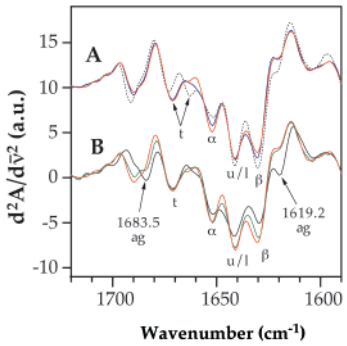

FIGURE 5: Temperature-dependent changes in the spectrum of the *Ss*EF-1α·GDP complex. (A) Dotted black, blue, and red curves represent the second-derivative spectra of the *Ss*EF-1α·GDP complex at 20, 75, and 80 °C, respectively. (B) Red, green, and black curves are those at 80, 90, and 98 °C, respectively. Symbols α, *β*, t, and u/l are defined in the legends of Figures 3 and 4; ag stands for absorption due to protein aggregation.

(Figure 1) which gave α-helix, *β*-sheet, and turn contents of 34, 40, and 14%, respectively. In addition, Table 1 shows that in the presence of NaCl the content of α-helix of the *Ss*EF-1α·GDP complex increased, while those of loops and/or unordered structures and *β*-sheets decreased. In the presence of NaBr or NH_4Cl, no significant changes in the *β*-sheets occurred, whereas an increase in the α-helix content was found, even though the extent was lower than that in the presence of NaCl. The effect of KCl on the *Ss*EF-1α secondary structure was negligible. Table 1 also shows the secondary structure composition of the *Ss*EF-1α·Gpp(NH)p complex in the absence or presence of 5 M NaCl. The α-helix (1651 cm^{-1} band) and turn (1664 cm^{-1} band) contents are higher and lower, respectively, than in the *Ss*EF-1α·GDP complex, in accordance with the second-derivative spectra shown in Figure 2B. On the contrary, Table 1 shows an increase in the *β*-sheet content (1631 cm^{-1} band) of the *Ss*EF-1α·Gpp(NH)p complex that was not revealed by second-derivative spectra (Figure 2B). This apparent discrepancy was due to the fact that the 1631 cm^{-1} band is slightly broader in the *Ss*EF-1α·Gpp(NH)p complex than in the *Ss*EF-1α·GDP complex, and therefore, a slightly higher *β*-sheet content in the former sample was determined. Also in this case, 5 M NaCl did not significantly affect the secondary structure content of the *Ss*EF-1α·Gpp(NH)p complex, different from what was observed in the case of the *Ss*EF-1α·GDP complex.

Thermal Stability of the SsEF-1α·GDP Complex. Protein denaturation following exposure to heat can be revealed in an FT-IR spectrum by a decrease in the intensity of α-helix and *β*-sheet bands, whereas aggregation, brought about by protein denaturation, is followed by the appearance and then the increase in intensity of two new bands close to 1620 and 1684 cm^{-1} (*29* and references therein). In the case of the *Ss*EF-1α·GDP complex, an unexpected phenomenon occurred. The increase in temperature from 20 to 70 °C caused a small decrease in the intensity of all amide I′ component bands; such a decrease was similar for all bands, thus indicating that no denaturation occurred within this temperature range (data not shown). Surprisingly, if the temperature was increased to 80 °C, the intensity of the α-helix band increased (Figure 5A), remained almost unchanged till 95 °C, and then started to decrease at 98 °C (Figure 5B). At this last temperature, the intensity of the *β*-sheet band decreased markedly and two new bands close to 1620 and 1684 cm^{-1} appeared, thus indicating that at 98 °C the *Ss*EF-1α·GDP complex started to undergo denaturation and aggregation.

Effect of the Bound Nucleotide or Salts on the Secondary Structure and Thermal Stability of SsEF-1α. The signal of the α-helix band in the second-derivative spectra of the *Ss*EF-1α·GDP complex was monitored in the absence or in the presence of different salts, as a function of temperature (Figure 6). In the absence of salts, the α-helix signal of both *Ss*EF-1α·GDP and *Ss*EF-1α·Gpp(NH)p complexes remained unchanged up to 70 °C; then, in the case of the *Ss*EF-1α·GDP complex, it increased to a maximum at 85−90 °C, whereas it decreased when the *Ss*EF-1α·Gpp(NH)p complex was considered instead. An increase in the α-helix signal from 45 to ∼65 °C was observed for the *Ss*EF-1α·GDP

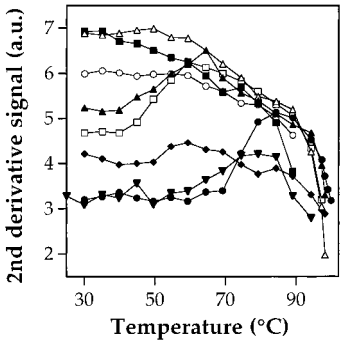

FIGURE 6: Temperature-dependent changes of the α-helix second-derivative signal for *Ss*EF-1α in the absence or presence of different salts at 20 °C. The second-derivative signals at 1651 cm^{-1} for the *Ss*EF-1α·Gpp(NH)p complex in the absence (◆) or presence (▼) of 5 M NaCl, the *Ss*EF-1α·GDP complex in the absence (●) or presence of 2.5 (▲) or 5 M NaCl (△), 2.5 M NaBr (■), 2.5 M KCl (□), or 2.5 M NH_4Cl (○) are reported.

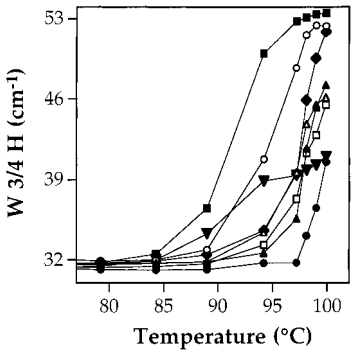

FIGURE 7: Thermal denaturation of *Ss*EF-1α in the absence or presence of different salts. The amide I′ bandwidth calculated at $^3/_4$ of the amide I′ band height (W 3/4 H) is reported for the *Ss*EF-1α·Gpp(NH)p complex in the absence (◆) or presence (▼) of 5 M NaCl, the *Ss*EF-1α·GDP complex in the absence (●) or presence of 2.5 M NaCl (▲), 5 M NaCl (△), 2.5 M NaBr (■), 2.5 M KCl (□), or 2.5 M NH_4Cl (○).

complex in the presence of 2.5 M NaCl or 2.5 M KCl, whereas in the presence of other salts, a continuous decay was observed. In addition, Figure 6 shows that, with the exception of nucleotide-bound *Ss*EF-1α in the absence of salts, the α-helix signal reached almost the same value at ∼60−65 °C and then it decreased in a similar way till protein denaturation. At ∼85 °C, the signal reached a value close to that of the *Ss*EF-1α·GDP complex in the absence of salts. Moreover, at 20 °C, NaCl at different concentrations and other salts provoked different increases in the α-helix content, which is consistent with the curve-fitting calculations reported in Table 1. With regard to the *β*-sheet signal (1631 cm^{-1}), it decreased with temperature in a similar way in all cases.

The onset of denaturation of the *Ss*EF-1α·GDP complex in the absence of salts occurred at ∼97 °C (Figure 7), and it was never complete. In the case of the *Ss*EF-1α·Gpp(NH)p complex, a significantly reduced thermostability was observed, even in the presence of 5 M NaCl; in fact, a T_m of ∼97 °C was found. It has to be noted that NaCl at 2.5 or 5 M affected the thermostability of the *Ss*EF-1α·GDP complex to an extent similar to that exerted by Gpp(NH)p, the T_m values being close to 98 or 97 °C, respectively. KCl at 2.5 M impaired the stability of the *Ss*EF-1α·GDP complex to an extent similar to that with 2.5 M NaCl. The highest destabilizing effect was observed at 2.5 M NaBr followed by that at 2.5 M NH_4Cl, and the corresponding T_m values were 91 and 94 °C, respectively. These data indicated that the destabilizing effect observed at high temperatures on *Ss*EF-1α depended on the cation, the anion, and the nucleotide bound as well.

DISCUSSION

In a previous paper, we reported that *Ss*EF-1α in the presence of NaCl at high concentrations displayed an intrinsic GTPase activity (*10*). This activity, which required the presence of $MgCl_2$ or $MnCl_2$, was not observed with chlorides of other monovalent cations such as Li^+, K^+, Rb^+, Cs^+, and NH_4^+. Other sodium salts (NaBr, $NaNO_3$, and CH_3COONa) were less efficient or not efficient at all (NaI and NaF). It was likely that the salts that were used produced on *Ss*EF-1α conformational changes responsible for the increased nucleotide hydrolysis activity. Therefore, an investigation regarding the effect of different salts on the secondary structure of the *Ss*EF-1α·GDP complex was undertaken, and the effect on the thermal stability of *Ss*EF-1α was also investigated. The experiments were carried out in the presence of Mg^{2+} and GDP; GTP could not be used because it is easily hydrolyzed at high temperatures or in the presence of sodium ions. To overcome this problem, in the absence of salts the slowly hydrolyzable GTP analogue Gpp(NH)p was used.

The FT-IR spectrum of the *Ss*EF-1α·GDP complex (Figure 1) and its deconvoluted (Figure 2A) and second-derivative transformation (Figure 2B) revealed that *Ss*EF-1α bound to either GDP or Gpp(NH)p is an α/*β* protein. The content of α-helices was somehow lower than that of *β*-sheets (Table 1). The total content of the secondary structure of the *Ss*EF-1α·GDP complex estimated by FT-IR measurements was very close to that derived from preliminary data on the 3D structure of the complex (unpublished results). The substitution of the GDP with Gpp(NH)p induced in *Ss*EF-1α a slight increase in the α-helix and *β*-sheet contents. These results are in line with those reported for eukaryotic EF-1α for which the great difference between the GDP- and GTP-bound forms, found in eubacterial EF-Tu (*5*, *6*), was not observed (*30*). In the presence of NaCl, the content of α-helix in the *Ss*EF-1α·GDP complex became significantly higher and that of unordered structures and/or loops and *β*-sheets decreased (Table 1). A small modification of the turns content was also observed in the presence of KCl, NaBr, and NH_4Cl. These findings indicated that a high ionic strength is resposible for such a behavior. It is interesting to note that, with the increase in temperature, the α-helix signal in the second-derivative spectra of the protein in the presence of different salts at 60 °C reached almost the same value. The signal then decreased and reached the same value as that of the *Ss*EF-1α·GDP complex in the absence of salts at ∼85 °C.

On the basis of the content of secondary structure, it was not possible to assign only to Na^+ the specific ability to trigger the $GTPase^{Na}$ since NH_4^+ and K^+, even though uneffective (*10*), caused an increase in α-helix content. In general, salts provoke a moderate effect on the content of *β*-sheets. In conclusion, the data in Table 1 indicate that the GTPase activity triggered by salts at high concentrations cannot be assigned to changes in the secondary structure of *Ss*EF-1α alone. On the other hand, the possibility that NaCl

stimulated the intrinsic GTPase of *Ss*EF-1α by inducing conformational changes in specific α-helix regions, similar to those found in the Gpp(NH)p-bound form of the enzyme (compare differences in intensity of the α-helix signal at ~1651 cm^{-1} reported in Figures 2 and 3), cannot be ruled out. In this context, besides small changes in the secondary structure, the infrared spectra revealed that (i) the *β*-sheets of the *Ss*EF-1α·Gpp(NH)p complex either in the absence or in the presence of NaCl display a better ability to undergo $^1H-^2H$ exchange than the *Ss*EF-1α·GDP complex does and (ii) the thermal stability of the Gpp(NH)p-bound form of *Ss*EF-1α is lower than that of the GDP-bound form. All together, these data suggest that the *Ss*EF-1α·Gpp(NH)p complex assumes in particular region(s) a conformation different from that present in the *Ss*EF-1α·GDP complex and NaCl is not able to induce the conformational changes observed when the nucleotide bound to *Ss*EF-1α was GDP.

The thermal denaturation profile of the *Ss*EF-1α·GDP complex in the absence of salts (Figure 7) showed that the T_m was higher than 100 °C. This value was at least 6 °C higher than that previously reported (*31*), and this finding can be ascribed to the fact that the *Ss*EF-1α concentration used in this work was 2 orders of magnitude higher. In addition, NaCl destabilized the overall protein structure to an extent that was much lower than that observed with NaBr or NH_4Cl (Figure 7). Via comparison of the destabilizing effect of 2.5 M NaBr with that of 2.5 M NaCl, it was clear that the stronger effect exerted by NaBr was due to the anion. The thermal denaturation of the *Ss*EF-1α·GDP complex evaluated in the presence of 2.5 M NH_4Cl, KCl, or NaCl assigned the highest destabilization effect to NH_4^+. Thus, the destabilizing effect of NaCl should be attributed to the charge density of Na^+, which affects the accessibility of the substrate into the catalytic site for GTP hydrolysis, and/or to the ability of the ions investigated to bind at specific sites of *Ss*EF-1α. The anion plays an important role in protein stability. In fact, NaBr triggered the *Ss*EF-1α GTPase to a level lower than that of NaCl (*10*). This finding can be attributed to a greater destabilizing effect of Br^- that would negatively affect the structure of the catalytic site for the hydrolysis of GTP. The breaking of hydrogen bonds or of salt bridges should also be considered, it having been reported that a high number of salt bridges plays an important role for the structural stability of thermophilic proteins at high temperatures (*32*, *33*).

REFERENCES

1. Masullo, M., Raimo, G., Parente, A., Gambacorta, A., De Rosa, M., and Bocchini, V. (1991) *Eur. J. Biochem. 199*, 529−537.
2. Bocchini, V., Adinolfi, B. S., Arcari, P., Arcucci, A., Dello Russo, A., De Vendittis, E., Ianniciello, G., Masullo, M., and Raimo, G. (1998) *Biochimie 80*, 895−898.
3. Raimo, G., Masullo, M., Lombardo, B., and Bocchini, V. (2000) *Eur. J. Biochem. 267*, 6012−6018.
4. Masullo, M., Ianniciello, G., Arcari, P., and Bocchini, V. (1997) *Eur. J. Biochem. 243*, 468−473.
5. Song, H., Parson, M. R., Rowsell, S., Leonard, G., and Phillips, S. E. V. (1999) *J. Mol. Biol. 285*, 1245−1256.
6. Bertchold, H., Reshetnikova, L., Reiser, C. O. A., Schirmer, N. K., Sprinzl, M., and Hilgenfeld, R. (1993) *Nature 365*, 126−132.
7. Kawashima, T., Berthet-Colominas, C., Wulff, M., Cusack, S., and Leberman, R. (1996) *Nature 379*, 511−518.
8. Nissen, P., Kjeldgaard, M., Thirup, S., Polekhina, G., Reshetnikova, L., Clark, B. F. C., and Nyborg, J. (1995) *Science 270*, 1464−1472.
9. Masullo, M., Raimo, G., and Bocchini, V. (1993) *Biochim. Biophys. Acta 1161*, 35−39.
10. Masullo, M., De Vendittis, E., and Bocchini, V. (1994) *J. Biol. Chem. 269*, 20376−20379.
11. Ianniciello, G., Masullo, M., Gallo, M., Arcari, P., and Bocchini, V. (1996) *Biotechnol. Appl. Biochem. 23*, 45−41.
12. Raimo, G., Masullo, M., and Bocchini, V. (1999) *FEBS Lett. 451*, 109−112.
13. Salomaa, P., Schaleger, L. L., and Long, F. A. (1964) *J. Am. Chem. Soc. 86*, 1−7.
14. Tanfani, F., Galeazzi, T., Curatola, G., Bertoli, E., and Ferretti, G. (1997) *Biochem. J. 322*, 765−769.
15. Banuelos, S., Arrondo, J. L. R., Goñi, F. M., and Pitaf, G. (1995) *J. Biol. Chem. 270*, 9192−9196.
16. Lee, D. C., Haris, P. I., Chapman, D., and Mitchell, R. (1990) *Biochemistry 29*, 9185−9193.
17. Chirgadze, Y. N., Fedorow, O. W., and Trushina, N. P. (1975) *Biopolymers 14*, 679−694.
18. Osborne, H. B., and Nabedryk-Viala, E. (1982) *Methods Enzymol. 88*, 676−680.
19. Arrondo, J. L. R., Muga, A., Castresana, J., and Goñi, F. M. (1993) *Prog. Biophys. Mol. Biol. 59*, 23−56.
20. Jackson, M., and Mantsch, H. H. (1992) *Biochim. Biophys. Acta 1118*, 139−143.
21. Krimm, S., and Bandekar, J. (1986) *Adv. Protein Chem. 38*, 181−364.
22. Tanfani, F., Lapathitis, G., Bertoli, E., and Kotyk, A. (1998) *Biochim. Biophys. Acta 1369*, 109−118.
23. Byler, D. M., and Susi, H. (1986) *Biopolymers 25*, 469−487.
24. Jackson, M., Haris, P. I., and Chapman, D. (1989) *Biochim. Biophys. Acta 998*, 75−79.
25. Reisdorf, W. C., and Krimm, S. (1996) *Biochemistry 35*, 1383−1386.
26. Heimburg, T., Schenemann, J., Weber, K., and Geisler, N. (1996) *Biochemistry 35*, 1375−1382.
27. Arrondo, J. L. R., and Goñi, F. M. (1999) *Prog. Biophys. Mol. Biol. 72*, 367−405.
28. Surewicz, W. K., Mantsch, H. H., and Chapman, D. (1993) *Biochemistry 32*, 389−394.
29. D'Auria, S., Barone, R., Rossi, M., Nucci, R., Barone, G., Fessas, D., Bertoli, E., and Tanfani, F. (1997) *Biochem. J. 323*, 833−840.
30. Negrutskii, B. S., and El'skaya, A. V. (1998) *Prog. Nucleic Acid Res. Mol. Biol. 60*, 47−78.
31. Arcari, P., Masullo, M., Arcucci, A., Ianniciello, G., de Paola, B., and Bocchini, V. (1999) *Biochemistry 38*, 12288−12295.
32. D'Auria, S., Moracci, M., Febbraio, F., Tanfani, F., Nucci, R., and Rossi, M. (1998) *Biochimie 80*, 949−957.
33. Ursby, T., Adinolfi, B. S., Al-Karadaghi, S., De Vendittis, E., and Bocchini, V. (1999) *J. Mol. Biol. 286*, 189−205.

BI0101291